Eur Biophys J (1989) 16:363–367

European Biophysics Journal

The dynamic properties of melittin in solution

Investigations by NMR and molecular dynamics

A. Pastore*, T. S. Harvey, C. E. Dempsey, and I. D. Campbell**

Department of Biochemistry, South Parks Road, Oxford, OX1 3QU, UK

Received June 13, 1988/Accepted in revised form September 2, 1988

Abstract. Molecular dynamics simulations are described for the peptide melittin. The atomic trajectories are calculated both with normal potential energy functions and with additional distance restraints deduced from nuclear Overhauser effects observed in NMR experiments. The results are compared with NMR data on coupling constants and amide exchange rates and with *B*-factors from X-ray crystallography. The observed correlations between experiment and molecular dynamics simulations suggest a relatively mobile *C*-terminus and relatively high flexibility around residue 11. It is noted that the high conformational variation around residue 11 is due in part to the presence of a proline at position 14 which results in a "missing" H-bond in the largely α-helical structure. It is also noted that a proline is a common feature of many putative membrane spanning helices. A role for such prolines is suggested.

Key words: NMR, molecular dynamics, hydrogen exchange, melittin, membrane proteins

I. Introduction

Calculations of the trajectories of the atoms in a protein under the influence of certain applied energy restraints have been used for a number of years to simulate the dynamics of the molecule (van Gunsteren et al. 1983; Kuriyan et al. 1986). The results have been correlated with experimental observables such as temperature factors in diffraction studies, and NMR data such as shifts and coupling constants (Dobson and Karplus 1986; van Gunsteren 1988) and hydrogen exchange (Levitt 1981). Over the last few years, molecular dynamics (MD) simulations have also been used in combination with NMR techniques to determine the 3D structure of macromolecules in solution (Scheek et al. 1985; Nilsson et al. 1986). An additional restraining potential energy function drives the molecule towards a conformation that satisfies distance restraints derived from NMR experiments.

Melittin is a membrane peptide of 26 residues. Under certain conditions it forms relatively stable, amphiphilic α-helices, a characteristic that is probably important for its biological activity (Tosteson and Tosteson 1981). The structure of melittin has been determined by X-ray crystallography (Terwilliger and Eisenberg 1982). The ^{1}H NMR spectrum of melittin in methanol has been completely assigned and the 3D structure has been calculated from the NMR restraints (Bazzo et al. 1988). In this solvent the peptide has a conformation similar to that in the crystal. In this paper the NMR restraints, molecular dynamics calculations and amide exchange rate data are used to explore the dynamic properties of melittin in solution. In particular the role of the proline at position 14 in the sequence is assessed. This proline occupies a position similar to that in many membrane spanning helices in transport proteins (Brandl and Deber 1986).

II. Simulations

All the energy minimization and molecular dynamics calculations were carried out using the GROMOS package of programs, kindly provided by W. F. van Gunsteren. The initial structures for the simulations were obtained using the crystallographic coordinates from the Brookhaven Protein Data Bank (one of the four molecules in the unit cell) or from structures generated from NMR data using the program DISSMAN (Terwilliger and Eisenberg 1982; Bazzo et al. 1988). Before starting the MD simulation the initial conformation was energy minimised (van Gunsteren and Karplus 1982).

* Present address: EMBL, Meyerhofstrasse 1, D-6900 Heidelberg, Federal Republic of Germany

** To whom offprint requests should be sent

In the MD, initial velocities for the atoms were taken from a random Maxwellian distribution at 293 K. The system was weakly coupled to a thermal bath of $T = 293$ K (Berendsen et al. 1984). When integrating the equations of motion with time step $t = 2$ fs, the algorithm was performed with temperature relaxation time $t = 0.01$ during the first 2 ps of equilibration and $t = 0.1$ thereafter (Aqvist et al. 1985). All bond lengths were kept rigid during the simulation by using the SHAKE algorithm (van Gunsteren and Berendsen 1977; Ryckaert et al. 1977). The simulation was performed without explicitly considering solvent molecules.

The 193 distance restraints from nuclear Overhauser effect data were applied in the restrained molecular dynamics (RMD) simulations as a semi-harmonic potential function with a force constant of 1000 kJ nm^{-2} mol^{-1} (van Gunsteren et al. 1985). This means that the extra potential energy term appears only if the actual distance between a restrained atom pair exceeds the limit imposed by the NMR data. The value of force constant chosen effectively allows a distance restraint violation of + 0.025 nm before a penalty at the level of kT occurs, and is consistent with the experimental accuracy of the NMR restraints (Kaptein et al. 1988) . It also allows some atomic motion while providing enough force to drive the molecule to a structure satisfying these restraints. Each MD trajectory covered a period of at least 60 ps but only the last 20 or 30 ps, when the molecule has attained an equilibrium, were considered.

III. Results

Most of the structural restraint data used in this paper have been taken from our previous NMR studies of melittin (Bazzo et al. 1988). Using the experimental nuclear Overhauser effect (nOe) restraints, five averaged RMD conformations were calculated. These are shown with a representative X-ray structure in Fig. 1. The calculated average structure of 110 ps of dynamics from the five trajectories has an average restraint violation of 0.004 nm. A best-fit program applied to the region from residue 2 to 9 was used to align the structures, considering only C_α atom positions (Kabsch 1976). An α-helical conformation between residues 1–11 and 12–26 is common to all six structures but the relative orientations of these helical regions varies between the structures. There appears to be a "hinge" in the molecule around residues 11 and 12. The dynamic nature of this bend or hinge will now be described in more detail.

Figure 2 is a plot of theta, the angle between the two sections of α-helix, against time (ps) for part of an RMD (A) and an unrestrained molecular dynamics

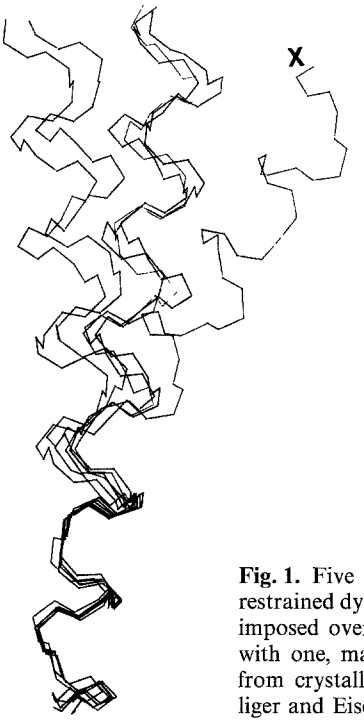

Fig. 1. Five structures from averaged restrained dynamics trajectories, superimposed over C_α atoms 2–9, together with one, marked with an X, derived from crystallographic studies (Terwilliger and Eisenberg 1982)

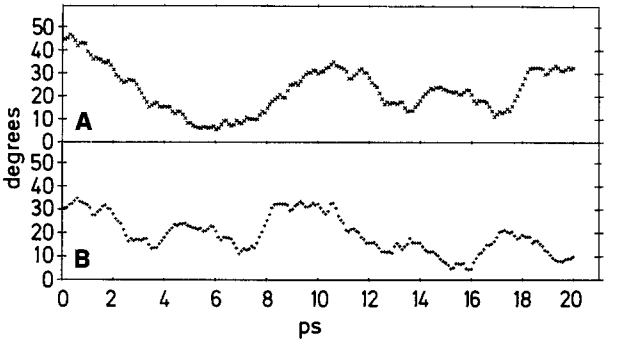

Fig. 2 A and B. The variation, with time, of theta, the angle between the α-helical sections comprising residues 2–10 and 14–25, for: **A** part of a restrained dynamics trajectory; **B** part of an unrestrained dynamics trajectory. The details of the simulations are decribed in the text

(UMD) trajectory (B). For the calculation of theta, four regions were defined, two in each helical section. These regions were residues 2 to 6, 7 to 11, 14 to 18 and 19 to 23. The centre of mass of each region was calculated and the two points obtained for each section of helix used to define a vector for the respective helical section. The angle between these two vectors was then calculated, and taken as the angle between the helices (Aqvist et al. 1985). A large variation in angle can be seen, around an average value of about 20°. Analysis of the molecule in an UMD trajectory showed similar behaviour. It should be noted that in the NMR experiments, strong $\alpha N(i, i+3)$ and $\alpha N(i, i+4)$ nOes were observed in the 2–9 and 16–26 regions of the mole-

cule. This kind of nOe was, however, too weak to detect in the 9–15 region. For example, the $\alpha N(i, i+3)$ from 9–12 and 11–14 were undetectable (the 10–13 cross peak position was obscured by overlap). The $\alpha N(i, i+4)$ nOes between 8–12, 9–13 and 11–15 were also too weak to observe. Thus the fact that RMD trajectories are no more restricted around the hinge region than UMD trajectories is a reflection of negative but real experimental information.

In addition to nOes there are further data which indicate the relative mobility of different regions of the melittin molecule. A comparison of the crystallographic *B*-factors with MD simulation data can be made. In the absence of disorder in the crystal, the *B*-factors are related to a root mean square (rms) fluctuation of the atomic coordinates (Frauenfelder et al. 1979). Figure 3 a, b and c compare the rms deviations for the C_α carbon atoms from the crystallographic data, the RMD and UMD trajectories. It may be noted that there is a correlation between the data suggesting an increase in mobility towards the *C*-terminus and around residue 11. As might be expected, the RMD trajectory explores less conformational space than the UMD trajectory.

Figure 4 a and b also show the rms fluctuations of the phi angles for both RMD and UMD runs. The region around residues 11 and 12 and the *C*-terminal regions again exhibit the largest variation. It is the variation of both φ and ψ for residues 11 and 12 that produces the changes in the angle between the two α-helical sections. In the RMD trajectories, the hinge is more sharply defined, while the *N*-terminal α-helical section becomes longer and more stable than in the UMD trajectories. Similarly, the *C*-terminal residues become less "mobile" upon the imposition of restraints.

Experimental evidence for conformational fluctuations that result in the breaking of hydrogen bonds may be obtained from hydrogen exchange data (Englander and Kallenbach 1984). The exchange process can be analysed in terms of the following scheme in which hydrogen exchange with solvent occurs from non-hydrogen bonded "open" conformers (N–H_o) in equilibrium with "native" hydrogen bonded conformers (N–H_c):

$$\text{N–H}_c \underset{k_1}{\overset{k_1}{\rightleftharpoons}} \text{N–H}_o \xrightarrow{k_3} \text{N–D}_o$$

In the case of melittin in methanol it has been shown that $k_2 \gg k_3$ (Dempsey 1988); this is known as the EX_2 limit (Englander and Kallenbach 1984) when the rate of amide exchange with solvent is given by:

$$k_{ex} = k_1 \cdot k_3 / k_2 = K_0 k_3$$

K_0 is the equilibrium constant that characterises the conformational fluctuations (N–$H_c \rightleftharpoons$ N–H_o). Values

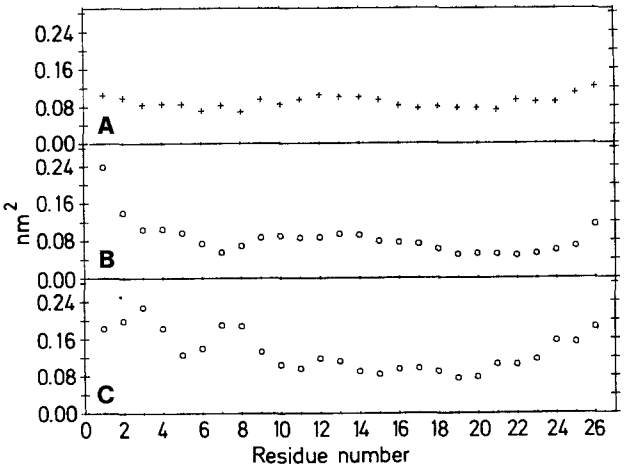

Fig. 3 A–C. The rms deviation of C_α atom positions as derived from: **A** the crystallographic *B*-factors (Terwilliger and Eisenberg 1982); **B** 110 ps restrained dynamics trajectories, and **C** 110 ps unrestrained dynamics trajectories

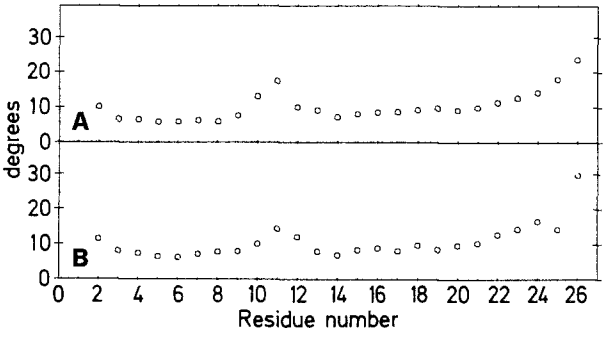

Fig. 4 A and B. The rms deviation of phi for each residue as calculated in 110 ps of molecular dynamics trajectories: **A** restrained; **B** unrestrained

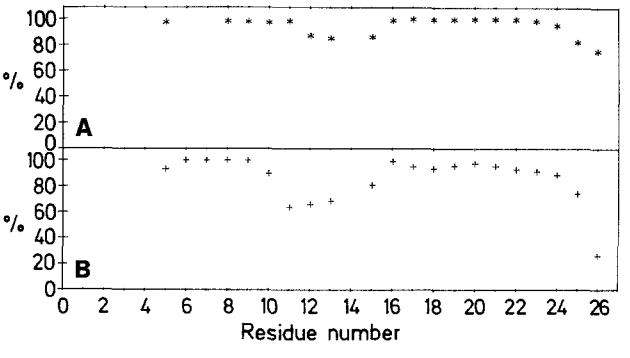

Fig. 5 A and B. Plots of: **A** the % lifetime of regular helical hydrogen bonds (NH_i to carbonyls CO_{i-4}), calculated from the restrained dynamics simulations; **B** the corresponding amide hydrogen lifetime calculated from the observed amide exchange rates as described in the text

of K_0 for the melittin amides can be calculated from published data (Dempsey 1988) by dividing the measured rate at the minimum of the pH-dependent exchange curve, k_{min}, by the observed minimum rate for Ala-4 NH which does not form an intramolecular hydrogen bond (Dempsey 1988; Bazzo et al. 1988); i. e. $k_{min}(\text{Ala-4}) = k_3$. A plot of the percentage lifetime of backbone hydrogen bonds, calculated from the K_0 values $\{100/(1+K_0)\%\}$ is shown in Fig. 5. The figure also shows that these percentages correlate strongly with the percentage time an amide hydrogen makes a regular hydrogen bond during a molecular dynamics simulation.

IV. Discussion

This dynamics study has proved successful in the correlation of simulated data with measured parameters. Using a chosen force constant, it has been possible to study the dynamics of melittin under conditions where the NMR restraints are of similar magnitude to other intra-molecular forces. It is interesting to note the agreement between results obtained using methods involving widely different time scales. The results presented here for backbone atoms provide good evidence that the *C*-terminus and the centre of the molecule, around residue 11, are relatively flexible.

Proline is unique among the common amino-acids in that both *cis*- and *trans*-forms are found and in that it cannot form an H-bond. In a helical structure this means that an H-bond to the amino acid four residues before the proline is missing. The presence of prolines in putative *trans*-membrane helices has been noted previously (Brandl and Deber 1986). This has led to various proposals for their role in *trans*-membrane proteins including a "proton motive force inducer" (Dunker 1982), exposure of a backbone carbonyl (Eisenman and Dani 1987), a kink or bend (Fox and Richards 1982) and *cis-trans* isomerism for the opening and closing of transport channels (Brandl and Deber 1986). Our NMR studies, however, indicate that prolines in similar peptide helices remain *trans* (Bazzo et al. 1988, Esposito et al. 1987, unpublished data). The current study suggests that prolines allow two helical segments to be formed within the membrane. There can be large changes in the relative orientation of the two helical segments which can occur quite rapidly. This flexibility is probably enhanced by the presence of a glycine a few residues before the proline. A study of putative *trans*-membrane helices suggests that the position of this flexibility would often coincide with the centre of the lipid bilayer. The possible variation in angle within a *trans*-membrane helix could be very important both in the assembly of a stable bundle of helices and in allowing such a bundle to accommodate the transport of a substrate.

Acknowledgements. We thank SERC, MRC, ICI and the Wellcome Trust for financial support.

References

Aqvist J, Gunsteren WF van, Leijonmarck M, Tapia O (1985) A molecular dynamics study of the C-terminal fragment of the L7/L12 ribosomal proton protein secondary structure in a 150 picosecond trajectory. J Mol Biol 183:461–477

Bazzo R, Tappin MJ, Pastore A, Harvey TS, Carver JA, Campbell ID (1988) The structure of melittin a ^{1}H-NMR study in methanol. Eur J Biochem 173:139–146

Berendsen HJC, Postma JPM, Gunsteren WF van, Di Nola A, Haak JM (1984) Molecular dynamics with coupling to an external bath. Proc Natl Acad Sci USA 81:3684–3690

Brandl CJ, Deber CM (1986) Hypothesis about the function of membrane-bound proline residues in transport proteins. Proc Natl Acad Sci USA 83:917–921

Dempsey CE (1988) pH dependence of hydrogen exchange from backbone peptide amides of melittin in methanol. Biochemistry 27:6893–6901

Dobson CM, Karplus M (1986) Nuclear magnetic resonance measurements and dynamical simulations. Methods Enzymol 131:362–371

Dunker AK (1982) A proton motive force transducer and its role in proton pumps, proton engines, tobacco mosaic virus assembly and hemoglobin allosterism. J Theor Biol 97:95–127

Eisenman G, Dani JA (1987) An introduction to molecular architecture and permeability of ion channels. Annu Rev Biophys Chem 16:205–226

Englander SW, Kallenbach N (1984) Hydrogen exchange and structural dynamics of proteins and nucleic acids. Rev Biophys 16:521–655

Esposito G, Carver JA, Boyd J, Campbell ID (1987) High-resolution ^{1}H-NMR study of the solution structure of alamethicin. Biochemistry 26:1043–1050

Fox RO, Richards FM (1982) A voltage-gated channel model inferred from the crystal structure of an alamethicin at 1.5 A resolution. Nature 300:325–330

Frauenfelder H, Petsko GA, Tsernoglou D (1979) Temperature-dependent X-ray diffraction as a probe of protein structural dynamics. Nature 280:558–563

Gunsteren WF van (1988) The role of computer simulation techniques in protein engineering. Protein Eng 2:5–13

Gunsteren WF van, Berendsen HJC (1977) Algorithms for macromolecular dynamics and constrained dynamics. Mol Phys 34:1311–1327

Gunsteren WF van, Karplus M (1982) Effect of constraints on the dynamics of macromolecules. Macromolecules 15: 1528–1544

Gunsteren WF van, Berendsen HJC, Hermans J, Hol WG, Postma JPM (1983) Computer simulation of dynamics of hydrated protein crystals and its comparison with X-ray data. Proc Natl Acad Sci USA 80:4315–4319

Gunsteren WF van, Boelens R, Kaptein R, Scheek RM, Zuiderweg ERP (1985) An improved restrained molecular dynamics technique to obtain protein tertiary structure from nuclear magnetic resonance data. In: Hermans J (ed) Molecular dynamics and protein structure. Polycrystal Book Service, P. O. Box 27, Western Springs, I/60558, USA, pp 92–99

Kabsch W (1976) A solution for the best rotation to relate two sets of vectors. Acta Crystallogr 32A:922–923

Kaptein R, Boelens R, Scheek RM, Gunsteren WF van (1988) Protein structures from NMR. Biochemistry 27:5389–5395

Kuriyan J, Petsko GA, Levy RM, Karplus M (1986) Effect of anisotropy and anharmonicity on protein crystallographic refinement. J Mol Biol 190:227–254

Levitt M (1981) Molecular dynamics of hydrogen bonds in bovine trypsin inhibitor protein. Nature 294:379–380

Nilsson L, Clore GM, Groenenborn AT, Bruenger AT, Karplus M (1986) Structure refinement of oligonucleotides by molecular dynamics with nuclear Overhauser effect interproton distance restraints: application to 5′ d(GCTACG)$_2$. J Mol Biol 188:455–475

Ryckaert JP, Ciccotti G, Berendsen HJC (1977) Numerical integration of the cartesian equations of motion of a system with constraints: molecular dynamics of n-alkanes. J Comp Phys 23:327–341

Scheek RM, Zuiderweg ERP, Boelens R, Gunsteren WF van (1985) The tertiary structure of the Lac repressor headpiece derived from nuclear magnetic resonance spectroscopy. In: Govil G, Khetzapol CL, Seran A (eds) Magnetic resonance in biology and medicine. McGraw Hill, New York, pp 293–303

Terwilliger TC, Eisenberg D (1982) The structure of melittin. 2. Interpretation of the structure. J Biol Chem 257:6016–6022

Tosteson MT, Tosteson DC (1981) The sting: Melittin forms channels in lipid bilayers. Biophys J 36:109–116